buildings

MDPI

Article

Digital Twin-Ready Regional Screening for Multi-Hazard Inspection Prioritization of Built Heritage in Fujian, China

Hong Tang [1] and Junjie Zhang [2,*]

[1] Department of Architecture and Civil Engineering, Fujian Forestry Vocational Technical College, 140 Jinshan Road, Yanping District, Nanping 353000, China
[2] Greenwich School & International Business School, Yunnan University of Finance and Economics, 237 Longquan Road, Wuhua District, Kunming 650221, China
* Correspondence: zhangjj@ynufe.edu.cn

Abstract

Heritage managers must decide where detailed building inspections should begin as environmental pressures change across large and diverse portfolios. This study develops a digital twin-ready regional screening framework linking official heritage inventories, dated climate and vegetation observations, and transparent inspection priorities. In Fujian, China, 917 traditional-village records and 64 protected ancient-building records were compiled, of which 914 and 62, respectively, matched 75 county-level areas. The analysis uses 9900 matched county-month environmental observations from 2014 to 2024. Four environmental domains are combined with recorded heritage concentration and tourism pressure. Alternative decision weights, six input and indicator tests, and 10,000 Monte Carlo weight draws assess ranking consistency. Xiapu (0.722), Wuyishan (0.689), and Yongtai (0.655) lead the baseline inspection list. Alternative weighting scenarios yield Spearman correlations of 0.845–0.970, while a recent-state update yields 0.944. Environmental-domain exclusions produce correlations of 0.922–0.980. The framework connects province-wide prioritization with county verification, targeted digital surveys, and subsequent Heritage Building Information Modeling (HBIM). Its dated records and repeatable update rules provide a practical basis for scheduling conservation inspections as new evidence becomes available.

Keywords: built heritage; traditional villages; multi-hazard screening; inspection prioritization; digital twin-ready conservation; HBIM; uncertainty analysis

Check for updates

Academic Editors: Alberto Sanchez-Lite, José Luis Fuentes-Bargues, Cristina Gonzalez-Gaya and Sara María Sánchez González

Received: 29 September 2026
Revised: 17 October 2026
Accepted: 21 October 2026
Published: 24 October 2026

Copyright: © 2026 by the authors. Licensee MDPI, Basel, Switzerland. This article is an open access article distributed under the terms and conditions of the Creative Commons Attribution (CC BY) license.

1. Introduction

Historic buildings and traditional settlements face environmental pressures that vary in intensity, timing, and location. Strong winds, intense rainfall, heat, persistent moisture, and vegetation changes can affect the same heritage landscape, while conservation teams must allocate a finite capacity for field inspection. Choosing where to investigate first is therefore a recurring management decision. Research has documented climate threats to cultural heritage and the growing importance of coordinated adaptation [1,2]. Studies of compound events also show why simultaneous environmental pressures need to be considered together rather than as isolated variables [3–5].

Digital documentation has transformed the way individual historic structures are recorded and assessed. Heritage Building Information Modeling (HBIM) connects measured geometry with historical and technical information [6,7], while scan-to-BIM and three-dimensional GIS extend that information into spatially referenced models [8]. Digital twins add a continuing relationship between physical observations, model updates, and decisions [9,10]. These advances

invite a further question for conservation authorities responsible for hundreds of dispersed sites: which locations should receive detailed digital acquisition first?

Recent research in Buildings has advanced the use of digital twins throughout building operation and maintenance [11] and mapped their growing relationship with heritage documentation [12]. HBIM-based conservation workflows increasingly incorporate structured expert and stakeholder information [13,14]. Repeat photogrammetry, knowledge graphs, multilevel models, vulnerability-oriented HBIM, federated data systems, and simulation tools enrich the assessment of individual heritage assets [15–20]. Regional inspection planning can build on these capabilities by identifying locations selected for subsequent detailed investigation.

That decision emerges before a new laser scan or condition survey is commissioned. Provincial administrations coordinate protection records and inspection priorities, while county departments and site managers hold much of the local information needed to act. A useful regional screening framework must therefore combine environmental change with registered heritage locations, preserve the date and origin of each observation, and translate the resulting ranking into a clear request for on-site verification. A repeatable screening layer can link the regional allocation of surveys to the detailed work that follows.

The Fujian application develops a digital twin-ready regional screening record that connects official heritage inventories to dated environmental observations through persistent county identifiers. Keeping environmental conditions, heritage concentration, and tourism pressure separate makes the source of each inspection-priority score clear and explains why the inspection order differs from a map of environmental hotspots. Alternative weighting scenarios and Monte Carlo draws describe how the leading candidates respond to changes in planning preferences. The resulting records provide a traceable connection from provincial screening to county verification, targeted digital capture, and asset-level HBIM diagnosis. This repeatable link between regional evidence and building-specific assessment constitutes the central contribution of the study.

2. Materials and Methods

2.1. Study Area and Heritage Evidence Base

Fujian Province combines a typhoon-exposed coastline with mountainous inland settlements and a substantial stock of recorded built heritage. The heritage inventory combines the first four provincial traditional-village lists issued by the Fujian Provincial Department of Housing and Urban-Rural Development and other responsible provincial authorities, together with the Eleventh Batch of Fujian Provincial Cultural Relics Protection Units and Protection Scopes issued by the People's Government of Fujian Province in 2026. The compiled source records contain 917 traditional-village entries and 64 protected ancient-building entries. Spatial studies have described the uneven distribution of traditional villages in Fujian and elsewhere in China, including the roles of terrain, accessibility, and settlement history [21–24]. Tourism adds a further dimension to the management of historic settlements [25].

The official inventories were harmonized to six-digit county-level administrative identifiers and joined to dated environmental observations. After geographic matching, the analytical portfolio comprises 75 counties or county-level districts, 914 village records, and 62 ancient-building entries. Table A1 reports the full matched inventory. Wind, precipitation, and temperature observations derive from the European Centre for Medium-Range Weather Forecasts ERA5-Land monthly reanalysis, distributed through the Copernicus Climate Change Service Climate Data Store. Vegetation observations derive from NASA LP DAAC's MODIS/Terra Vegetation Indices Monthly L3 Global 1 km SIN Grid, Version 6.1 (MOD13A3). The harmonized environmental series covers 2014–2024 and contains

10,824 Fujian county-month observations, including 9900 observations for the 75 matched heritage areas. Table 1 summarizes the data sources, temporal and spatial coverage, and analytical roles of the principal datasets.

Table 1. Data sources, analytical support, and roles.

Source/Product	Temporal Support	Spatial Support	Core Fields	Analytical Role
Fujian provincial traditional-village lists, Batches 1–4 (Fujian Provincial Department of Housing and Urban-Rural Development et al.)	2015–2021	Village record, aggregated to county	917 official list records	Heritage exposure
Eleventh Batch of Fujian Provincial Cultural Relics Protection Units and Protection Scopes (People's Government of Fujian Province)	Approved 2025; published 2026	Protected building, aggregated to county	64 ancient-building entries	Heritage exposure
ERA5-Land monthly averaged data (ECMWF/C3S Climate Data Store)	2014–2024, monthly	County-month after spatial aggregation	10 m wind, total precipitation, 2 m air temperature	Environmental screening update
MODIS/Terra MOD13A3 V061 (NASA LP DAAC)	2014–2024, monthly	County-month after spatial aggregation	NDVI	Environmental stress
Official county statistical yearbooks and annual statistical communiqués	2013–2024; latest observed value	County	Tourism revenue, 10,000 CNY	Human-use pressure

Note: The ancient-building component uses the 64 ancient buildings in the eleventh provincial protection batch, while traditional-village counts use the four official provincial list releases included in the study. ERA5-Land and MOD13A3 were spatially aggregated to county-month units; MOD13A3 NDVI is reported after applying the 0.0001 scale factor.

2.2. Data Architecture and Institutional Update Responsibilities

Each county in the regional screening register has a persistent identifier and a dated record of its heritage inventory, environmental indicators, tourism pressure, and inspection-priority score. Equation (1) defines the updateable state vector, while Table 2 specifies the source, refresh cycle, and conservation use of each field. Retaining these linked records makes it possible to compare successive screening rounds and transfer a selected county to more detailed site and building assessments.

$$\mathbf{S}_i^{(w)} = \left(H_i^W, H_i^R, H_i^{HW}, H_i^E, E_i, T_i\right) \quad (1)$$

Table 2. Regional screening fields and update rules.

Field	Meaning	Update Class	Information Content	Primary Source
H^W	Wind state	Dynamic	Extreme-wind frequency and wind–rain concurrence	ERA5-Land, C3S Climate Data Store
H^R	Heavy-rain state	Dynamic	Extreme-rain frequency and wind–rain concurrence	ERA5-Land, C3S Climate Data Store
H^{HW}	Heat–wet state	Dynamic	Extreme-heat frequency and heat–rain concurrence	ERA5-Land, C3S Climate Data Store
H^E	Environmental stress	Dynamic	Low-NDVI frequency and negative NDVI trend	MODIS/Terra MOD13A3 V061, NASA LP DAAC
E	Heritage exposure	Inventory update	Traditional-village and ancient-building concentration	Official Fujian provincial heritage lists
T	Tourism pressure	Periodic	Latest observed county tourism revenue	Official county statistical yearbooks and annual statistical communiqués
P	Inspection priority	Derived each update	Weighted state score with uncertainty distribution	Derived from the preceding state variables

Note: A single county identifier links official inventories, periodically refreshed environmental evidence, and a versioned inspection-priority record. Detailed building surveys and HBIM assessments are linked through separate asset identifiers.

In Equation (1), county i at update window w has a state vector composed of wind stress H^W, heavy-rain stress H^R, heat–wet stress H^{HW}, environmental stress H^E, heritage exposure E, and tourism pressure T. ERA5-Land and MOD13A3 supply dated environmental refreshes; new provincial heritage lists revise E, and new officially reported tourism statistics revise T. Each refresh is linked to its source, date, geographic unit, and generated ranking, allowing a later inspection record to be related to the screening state that prompted it.

The framework follows the administrative responsibilities through which heritage information is collected and used. National authorities establish the principal conservation rules; the Fujian provincial government and its cultural-heritage administration coordinate provincial protection records; prefecture-level departments consolidate information across counties; and county-level offices and site managers verify conditions and prepare site-specific actions. A county-level district is treated as an equivalent administrative unit in the analysis. The provincial cultural-heritage administration is the proposed steward of the shared screening register. Heritage and housing authorities would provide inventory updates, climate and vegetation products would refresh the environmental fields, and county offices would link inspection records to individual assets. The revised Law of the People's Republic of China on the Protection of Cultural Relics, effective in March 2025, provides the legal context for these responsibilities. This sequence places province-wide prioritization and building-level assessment at clearly defined stages of conservation management.

2.3. Environmental Screening States and Compound Events

The environmental component uses four monthly measures: wind, precipitation, air temperature, and vegetation condition. Wind, rainfall, and temperature are drawn from the ERA5 reanalysis framework [26] and its land-focused ERA5-Land implementation [27]. Vegetation is measured with MOD13A3 NDVI, following the established interpretation of MODIS vegetation indices [28]. These four inputs describe complementary aspects of the environment surrounding recorded heritage and can be updated on a common monthly schedule.

Extreme monthly observations are defined relative to the pooled Fujian county-month distribution. Wind, precipitation, and temperature extremes occur above the corresponding 90th percentile; low vegetation condition occurs below the 10th percentile of scaled NDVI. The resulting thresholds are 2.999 m s^{-1}, 294.085 mm, 26.926 °C, and 0.496, respectively. MOD13A3 NDVI values are multiplied by the published 0.0001 scale factor before analysis. A consistent empirical-quantile rule is used throughout [29]. Equation (2) defines the indicators, and Table A2 reports their thresholds and interpretation.

$$I_{it}^{x} = \mathbb{1}\left(x_{it} \geq q_{0.90}^{x}\right), \quad x \in \{W, R, \Theta\}; \qquad I_{it}^{V} = \mathbb{1}\left(V_{it} \leq q_{0.10}^{V}\right) \tag{2}$$

Equation (2) uses the indicator function $\mathbb{1}(\cdot)$. Equation (3) then converts monthly extreme states into county-level event frequencies, where n_i is the number of valid monthly observations for county i.

$$F_i^x = \frac{1}{n_i} \sum_{t=1}^{n_i} I_{it}^x \tag{3}$$

Equation (4) captures compound occurrence through the monthly intersection of relevant states. Wind–rain concurrence identifies months with simultaneous extreme wind and heavy rainfall, while heat–rain concurrence identifies simultaneous extreme heat and heavy rainfall.

$$C_i^{WR} = \frac{1}{n_i} \sum_t I_{it}^W I_{it}^R, \qquad C_i^{\Theta R} = \frac{1}{n_i} \sum_t I_{it}^\Theta I_{it}^R \tag{4}$$

Equation (5) converts each county-level frequency or trend to an empirical percentile rank across the 75 matched heritage counties. This common 0–1 support preserves ordering while preventing indicators with long-tailed physical units from dominating the composite state. Rank agreement in the sensitivity analysis is evaluated with Spearman's coefficient [30].

$$Q(z_i) = \frac{r(z_i) - 1}{N - 1} \tag{5}$$

Equations (6)–(9) combine normalized observations into four environmental domains. Wind stress includes extreme-wind occurrence and its coincidence with heavy rainfall. Rainfall stress combines extreme precipitation with the observed rainfall trend. Heat–wet stress captures extreme temperature and its coincidence with rainfall, while environmental stress incorporates low NDVI and vegetation change. Equation (10) averages these four domains. The separate component scores remain available alongside the aggregate, allowing readers and managers to identify the pressures responsible for a county's position.

$$H_i^W = 0.65Q\left(F_i^W\right) + 0.35Q\left(C_i^{WR}\right) \tag{6}$$

$$H_i^R = 0.65Q\left(F_i^R\right) + 0.35Q\left(C_i^{WR}\right) \tag{7}$$

$$H_i^{HW} = 0.55Q\left(F_i^{\Theta}\right) + 0.45Q\left(C_i^{\Theta R}\right) \tag{8}$$

$$H_i^E = 0.60Q\left(F_i^V\right) + 0.40Q\left(-\hat{\beta}_i^V\right) \tag{9}$$

The mean in Equation (10) describes the environmental screening state. Heritage concentration and human-use pressure enter only at the subsequent prioritization stage, retaining separate interpretations for hazard, exposure, and decision context.

$$H_i = \frac{1}{4}\left(H_i^W + H_i^R + H_i^{HW} + H_i^E\right) \tag{10}$$

2.4. Heritage Exposure and Tourism Pressure

Heritage exposure is represented by a composite of official traditional-village and ancient-building record counts. Equation (11) applies a logarithmic transformation to the two count variables, reducing the effect of strongly concentrated registries, and places a coefficient of 0.45 on the more narrowly covered building inventory. This coefficient is a declared design choice that is assessed through alternative prioritization scenarios. The measure identifies the concentration of recorded heritage assets available for regional inspection planning.

$$E_i = Q\left[\ln(1 + V_i) + 0.45\ln(1 + B_i)\right] \tag{11}$$

In Equation (11), V_i denotes traditional-village records in the first four provincial lists and B_i denotes ancient buildings in the eleventh provincial protection batch. Equation (12) uses the most recent tourism-revenue figures reported in county statistical yearbooks and annual statistical communiqués. Observed tourism revenue is available for 50 of the 75 matched counties. Values are log-transformed and percentile-ranked; the remaining counties receive the portfolio median in the baseline. Additional assignments and an exclusion of tourism from the score are examined in Table A6 and Figure A2.

$$T_i = \begin{cases} Q\left[\ln(1 + Y_i)\right], & Y_i \text{ observed}, \\ \tilde{T}, & Y_i \text{ unavailable}, \end{cases} \tag{12}$$

2.5. Multi-Criteria Inspection-Priority Score and Decision Scenarios

Equation (13) combines the environmental state, recorded heritage concentration, and tourism pressure into an inspection-priority score. The baseline weights of 0.50, 0.35, and 0.15 are specified planning assumptions, not empirically calibrated conservation preferences. They place the greatest emphasis on environmental screening, followed by recorded heritage concentration and tourism-related use. A higher score indicates an earlier place in the schedule for verification, inspection, and detailed digital documentation. Research on composite indicators motivates explicit examination of weighting and aggregation decisions [31].

$$P_i = 0.50H_i + 0.35E_i + 0.15T_i \tag{13}$$

We compare the baseline ranking with balanced weights (0.40, 0.40, 0.20), hazard-heavy weights (0.65, 0.25, 0.10), heritage-heavy weights (0.35, 0.50, 0.15), and a tourism-free score (0.60, 0.40, 0.00). Six further scenarios test lower and upper tourism assignments for counties without observations and remove each environmental domain in turn. Rank correlation, top-ten overlap, and median absolute rank displacement are assessed together. This combination distinguishes broad portfolio agreement from shifts among the counties most likely to receive inspections first.

2.6. Weight Uncertainty, Inspection-Rank Stability, and State Updating

The Monte Carlo analysis evaluates how the ranking responds to variation in the three outer decision weights. The design uses 10,000 reproducible draws, following established uncertainty-sampling methods [32] and sensitivity-analysis principles [33]. Equation (14) draws weight vectors from a Dirichlet distribution centered on (0.50, 0.35, 0.15), with concentration 40. Equation (15) recomputes each county's score for every draw.

$$\mathbf{w}^{(b)} \sim \text{Dirichlet}(\kappa \mathbf{w}_0), \quad \mathbf{w}_0 = (0.50, 0.35, 0.15), \quad \kappa = 40, \quad b = 1, \ldots, 10,000 \tag{14}$$

$$P_i^{(b)} = w_H^{(b)} H_i + w_E^{(b)} E_i + w_T^{(b)} T_i \tag{15}$$

For every county, the simulated scores yield a median rank, a central 90% rank interval, and the probability of appearing in the leading 10 or 20 positions. We present these measures alongside the deterministic scenarios, consistent with recommendations to examine the robustness of composite indicators across assumptions [34].

The dynamic component is illustrated by updating the environmental domains with observations from 2022 to 2024 while holding heritage records, latest reported tourism states, and outer weights fixed. The revised scores can then be compared with the 2014–2024 baseline. The same procedure can be repeated when a new monitoring period or an updated administrative inventory becomes available.

3. Results

3.1. Heritage Inventory and Environmental Screening States

The matched portfolio covers 75 county-level areas, with 914 registered traditional-village records and 62 ancient buildings. The average county has 12.19 village records (interquartile range 5–19; maximum 47) and 0.83 protected ancient buildings (maximum eight). Of the 9900 matched county-month observations, the average county frequency is 0.096 for extreme rainfall and 0.085 for both high wind and high temperature. Table 3 reports the distribution of the main inputs and scores.

Table 3. Descriptive statistics for the heritage-county screening indicators.

Variable	N	Mean	SD	P25	Median	P75	Max
Traditional-village records	75	12.187	10.847	5.000	8.000	19.000	47.000
11th-batch ancient buildings	75	0.827	1.329	0.000	0.000	1.000	8.000
Total recorded heritage entries	75	13.013	10.987	5.000	9.000	19.000	47.000
Extreme-wind frequency	75	0.085	0.185	0.000	0.000	0.011	0.758
Extreme-rain frequency	75	0.096	0.034	0.080	0.098	0.114	0.174
Extreme-heat frequency	75	0.085	0.078	0.011	0.068	0.125	0.265
Low-NDVI frequency	75	0.047	0.144	0.000	0.000	0.015	1.000
Wind–rain concurrence	75	0.002	0.006	0.000	0.000	0.000	0.038
Heat–rain concurrence	75	0.006	0.011	0.000	0.000	0.011	0.038
Environmental screening score	75	0.507	0.142	0.396	0.477	0.585	0.820
Heritage-exposure score	75	0.507	0.290	0.280	0.513	0.753	1.000
Tourism-pressure score	75	0.510	0.237	0.390	0.510	0.630	1.000
Baseline priority score	75	0.507	0.096	0.437	0.508	0.578	0.722
2022–2024 updated priority	75	0.507	0.101	0.437	0.516	0.582	0.757

Note: Frequency variables represent the share of valid county-month observations. Environmental states, heritage exposure, tourism pressure, and inspection scores are normalized to comparable relative supports.

Environmental conditions and heritage concentration follow different geographic patterns. Coastal counties more often receive high wind or rainfall scores, whereas several inland counties contain larger concentrations of recorded heritage. Figure 1 displays the four environmental domains, heritage exposure, tourism pressure, and resulting inspection score for the 40 highest-ranked counties. The labeled cells make it possible to see which component raises a location's priority.

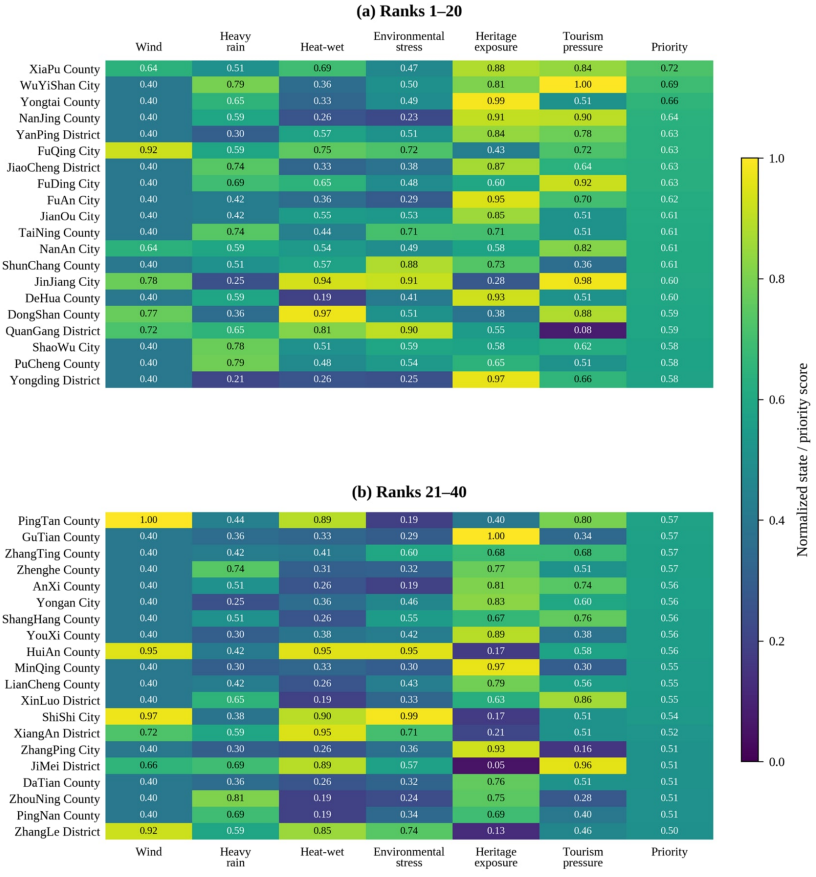


Figure 1. Component signatures for the 40 highest baseline inspection priorities. Panels (**a**,**b**) report ranks 1–20 and 21–40. All values are provided on a common 0–1 scale, with each cell labeled numerically; the full 75-county matched inventory is presented in Table A1.

3.2. Inspection Priorities Versus Hazard Concentration

Huian has the highest composite environmental-state score (0.820), followed by Shishi (0.811), Xiuyu (0.792), Changle (0.776), Quangang (0.771), and Licheng (0.767). The inspection ranking differs because it also accounts for registered heritage concentration and tourism pressure. Xiapu ranks first (0.722), followed by Wuyishan (0.689) and Yongtai (0.655); Nanjing and Yanping complete the leading five. Figure 2a locates counties by environmental state and heritage concentration. Figure 2b compares the final inspection order with the hazard-only ranking, while Table 4 reports the 20 highest-ranked counties.

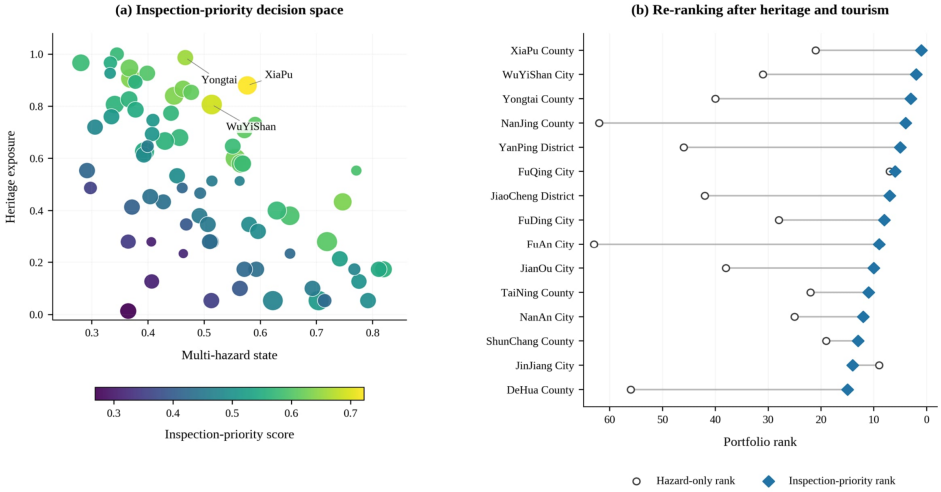


Figure 2. Multi-criteria inspection decisions across the heritage portfolio. (**a**) Joint environmental and heritage exposure states for the 75 counties, with marker size representing tourism pressure and color indicating inspection priority. (**b**) Changes from hazard-only ranks to multi-criteria inspection-priority ranks for the leading 15 counties.

Table 4. The 20 highest-ranked counties under the baseline inspection-priority score.

Rank	County	Village Records	Ancient Buildings	Hazard	Heritage	Tourism	Priority	P(top 10)
1	Xiapu County	19	3	0.577	0.880	0.840	0.722	100.0%
2	Wuyishan City	16	2	0.514	0.807	1.000	0.689	99.7%
3	Yongtai County	47	0	0.466	0.987	0.510	0.655	90.1%
4	Nanjing County	31	1	0.369	0.907	0.900	0.637	72.9%
5	Yanping District	22	1	0.447	0.840	0.780	0.634	83.9%
6	Fuqing City	9	0	0.747	0.433	0.720	0.633	69.4%
7	Jiaocheng District	34	0	0.463	0.867	0.640	0.631	75.9%
8	Fuding City	13	0	0.556	0.600	0.920	0.626	66.7%
9	Fuan City	45	0	0.367	0.947	0.700	0.620	52.2%
10	Jianou City	14	5	0.477	0.853	0.510	0.614	46.2%
11	Taizhu County	7	8	0.572	0.707	0.510	0.610	14.1%
12	Nanan City	9	1	0.566	0.580	0.820	0.609	31.4%
13	Shunchang County	13	2	0.591	0.733	0.360	0.606	26.9%
14	Jinjiang City	5	0	0.719	0.280	0.980	0.604	43.0%
15	Dehua County	26	2	0.399	0.927	0.510	0.600	26.7%
16	Dongshan County	5	1	0.652	0.380	0.880	0.591	20.9%
17	Quangang District	7	2	0.771	0.553	0.080	0.591	27.8%
18	Shaowu City	9	1	0.569	0.580	0.620	0.580	0.0%
19	Pucheng County	19	0	0.551	0.647	0.510	0.578	0.0%
20	Yongding District	34	1	0.281	0.967	0.660	0.578	9.7%

Note: P(top 10) is calculated from 10,000 Monte Carlo weight draws. County names are presented in English administrative form throughout the manuscript and Appendix A.

3.3. Weight-Induced Rank Stability Among Leading Inspection Candidates

The Monte Carlo experiment identifies leading candidates whose inspection rank remains stable across alternative decision weights. Xiapu appears in the top ten in every draw, with a central 90% rank interval of 1–1. Wuyishan remains in ranks 2–4 and appears in the top ten in 99.7% of draws. Yongtai has a wider rank interval of 2–14 and a 90.1% top-ten probability. Figure 3 presents the intervals beside the corresponding top-ten probabilities; Table A4 reports these statistics for 25 counties.

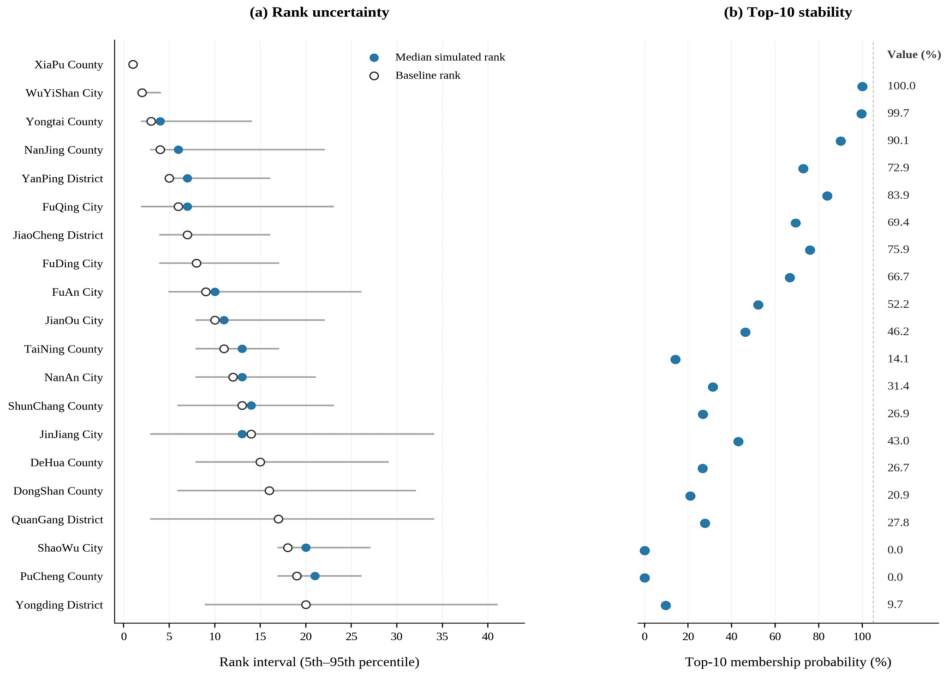


Figure 3. Stability of the 20 leading inspection priorities under 10,000 Monte Carlo weight draws. (**a**) Baseline and simulated median ranks with the 5th–95th percentile interval. (**b**) Top-10 membership probability, with all numerical percentages aligned in a separate value column.

3.4. Alternative Criteria and Data Treatments Preserve Substantial Ranking Concordance

The alternative weights preserve substantial agreement across the full 75-county ranking. Spearman correlations are 0.970 under balanced weights, 0.845 with greater environmental emphasis, 0.899 with greater heritage emphasis, and 0.931 when tourism is omitted. Updating the environmental state to 2022–2024 produces a correlation of 0.944. Figure 4 shows the complete scenario ranks for the baseline top 25, while Table 5 reports the five main comparisons. Table A6 extends the analysis to tourism-data assignments and environmental-domain exclusions, reporting both rank agreement and top-ten overlap.

Table 5. Rank sensitivity relative to the baseline model.

Scenario	Environmental/Heritage/Tourism Weights	Spearman ρ	Purpose
Balanced	0.40/0.40/0.20	0.970	Tests equal emphasis on hazard and heritage
Hazard-heavy	0.65/0.25/0.10	0.845	Tests stronger environmental screening
Heritage-heavy	0.35/0.50/0.15	0.899	Tests concentration-led conservation
No tourism	0.60/0.40/0.00	0.931	Removes the incomplete tourism term
Recent state	0.50/0.35/0.15	0.944	Updates the 2014–2024 environmental state to 2022–2024

Note: The recent-state row uses the baseline outer weights and updates only the environmental state. All reported correlations are between full 75-county rank vectors.

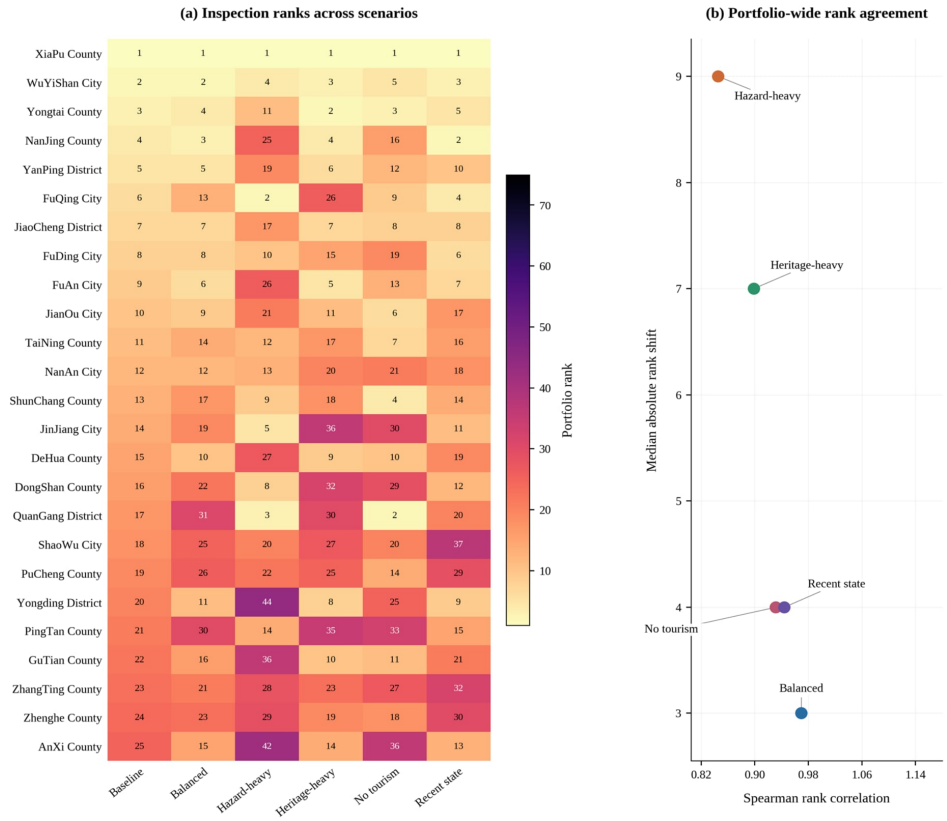


Figure 4. Sensitivity of inspection-priority order. (**a**) Rank of each baseline top-25 county under alternative weights, tourism treatment, and recent-state updating; all cells contain exact rank values. (**b**) Portfolio-wide Spearman agreement and median absolute rank displacement, with separated scenario labels.

3.5. Recent-State Updates to Inspection Priorities

Updating the environmental layer with observations from 2022 to 2024 gives a Spearman rank correlation of 0.944 relative to the 2014–2024 baseline. Xiapu remains first, while Nanjing moves from fourth to second and Wuyishan from second to third. Yongding rises from twentieth to ninth and Anxi from twenty-fifth to thirteenth; Shaowu moves from eighteenth to thirty-seventh and Jianyang from forty-fifth to sixty-fourth. The county-specific changes show how dated environmental information can revise the order of candidates considered for detailed inspections while preserving substantial agreement across the wider portfolio.

Counties with similar total scores can reach them through different combinations of evidence. Xiapu has high recorded heritage concentration and tourism pressure alongside above-median environmental stress. Wuyishan combines strong tourism pressure with very high heritage concentration; Yongtai ranks highly mainly because it contains the largest number of traditional-village records. Figure 5 decomposes the scores into labeled weighted contributions and plots their relative composition, supporting a more informative interpretation than the final rank alone.

The Appendix A provides the underlying details in the order cited here. Table A1 lists the matched heritage inventory, Table A2 the environmental thresholds, Table A3 the leading component scores, Table A4 the Monte Carlo rank distributions, Table A5 the largest rank changes after the recent-state update, and Table A6 the additional sensitivity scenarios. Figure A1 presents monthly environmental conditions, and Figure A2 compares inspection scores with and without tourism. Equations (A1) and (A2) define rank change and rank concordance, respectively.

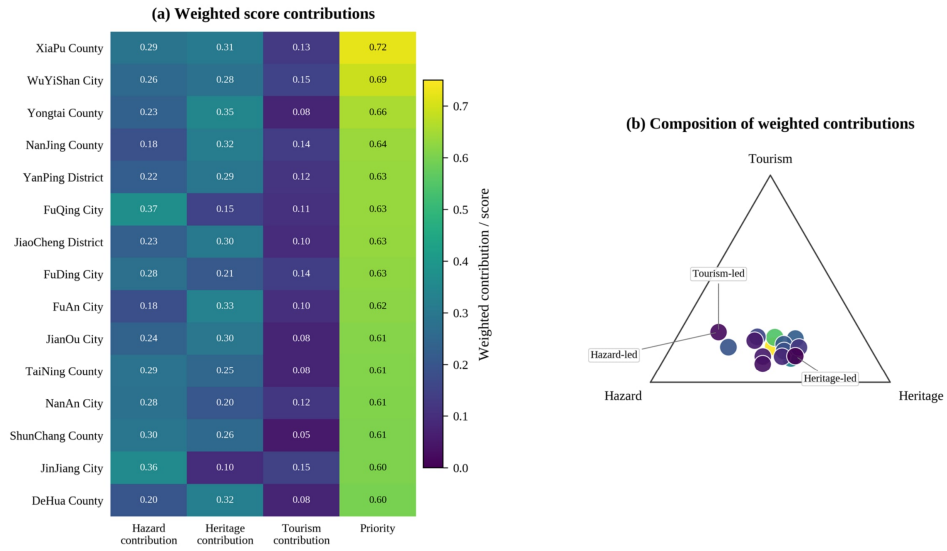


Figure 5. Contributions to the baseline top-15 inspection priorities. (**a**) Hazard, heritage, and tourism contributions to the composite inspection score, with all cells numerically labeled. (**b**) Relative composition of the three contributions; marker size and color represent total inspection priority.

4. Discussion

4.1. The Scientific Contribution of Regional Screening

The main contribution is a province-wide screening layer that joins official heritage inventories to dated environmental evidence and then identifies locations for detailed surveys. Building-scale research demonstrates the value of laser scanning and BIM for heritage documentation [35] and uses HBIM to connect asset information with engineering evaluation [36]. The present framework addresses the earlier portfolio decision: where should time-consuming survey and digital acquisition begin? Persistent county identifiers, known source dates, and repeatable update rules make that decision traceable across successive monitoring periods.

A review involving Xekalakis and colleagues [37] connects crowdsourced records, laser scanning, and HBIM to progressively more detailed heritage assessment. Regional screening adds a complementary first stage. Environmental records identify changing pressures, administrative registers locate the heritage requiring attention, and rank diagnostics explain how planning preferences affect the inspection schedule. These dated screening records can then accompany site-specific survey and modeling activities.

4.2. Why Environmental Hotspots and Heritage Inspection Priorities Differ

Environmental hotspots and inspection priorities need not coincide. Research on large infrastructure portfolios shows the importance of combining environmental stress with asset exposure [38]; studies of flood-related heritage vulnerability likewise distinguish physical threats from the properties of exposed buildings [39]. In Fujian, the highest environmental-state scores occur in several coastal districts, whereas the combined inspection score places Xiapu, Wuyishan, and Yongtai at the top for different reasons. This distinction is consequential when deciding where to deploy specialist survey teams.

National-scale analyses of climate threats to Chinese cultural heritage underline the value of connecting environmental observations to conservation decisions [40]. The Fujian results provide that connection through a dated screening record, a transparent county ranking, and a defined route to asset-level investigation. The framework is designed for heritage portfolios where sites are widely dispersed and survey effort must be sequenced.

4.3. Governance and Practical Conservation Pathways

Effective heritage adaptation depends on sound information, institutional coordination, and the ability to turn observations into conservation activity [41]. Assessments of World Heritage exposed to climate pressures also show why local circumstances matter [42]. For Fujian, the results suggest a differentiated inspection program: coastal locations with high wind and rainfall states can be reviewed after relevant events, while inland heritage concentrations can be considered for planned condition surveys and inventory updates. This makes the regional ranking useful to both provincial coordinators and local conservation offices.

The proposed handoff follows three stages. The provincial cultural-heritage administration maintains the common screening record and circulates ranked candidates for technical review. Prefecture and county offices verify inventory information, arrange site visits, and identify buildings requiring digital capture. Site managers and conservation professionals then undertake HBIM documentation, structural diagnosis, and intervention planning as appropriate. Inspection outcomes can be linked back to the regional record and used in subsequent screening rounds. Research on heritage disaster management and adaptation supports this coordinated approach [43,44].

4.4. Connecting Regional Screening with Asset-Level Heritage Digital Twins

The register also provides a common identifier structure for adding finer information as it becomes available. Sentinel-1 can inform surface-change monitoring [45], and Dynamic World supplies frequently updated land-cover probabilities [46]. Scalable geospatial processing [47] and mapped surface-water histories [48] can enrich the environmental context around individual heritage locations. Such extensions would retain a link to the same county and asset identifiers used in the screening record.

Coastal hazard screening can be developed further with storm-track information from the International Best Track Archive for Climate Stewardship [49]. For buildings selected for detailed study, heritage-science research emphasizes bringing together geometry, construction history, material properties, and condition surveys within HBIM [50]. The proposed information structure gives these higher-resolution studies a clear administrative entry point and keeps inspection decisions connected to their supporting regional evidence.

4.5. Positioning the Framework Within the State of the Art

Sevieri et al. [51] developed a multi-level framework in which progressively detailed surveys improve the prioritization of cultural-heritage assets. Sugiyama et al. [52] examined how the information content and functions of a Heritage Digital Twin can be assessed. This study connects these approaches at the provincial scale: a time-stamped regional screening record identifies inspection candidates, describes the evidence behind their rankings, and connects them to subsequent asset documentation. The resulting contribution lies in this repeatable connection between regional selection and building-level investigation.

The rankings retain broad agreement under the principal alternatives. Removing tourism yields Spearman $\rho = 0.931$, and the recent-state update yields 0.944. Environmental-domain exclusions yield 0.922–0.980 (Table A6), while the baseline first-ranked county remains in the top two in the six supplementary scenarios. Figure A2 compares the tourism-free and baseline scores. Together, these results support an inspection sequence that can be revisited transparently as new information becomes available.

4.6. Limitations

The county-scale screening combines monthly environmental observations, official heritage inventories, and tourism statistics available for 50 of the 75 matched counties.

Condition surveys, construction materials, measured deterioration, prospective damage, intervention costs, and restoration feasibility are addressed in subsequent site-level assessments. Alternative tourism assignments change some positions in the leading inspection tier, and the weight simulations assess the three specified planning coefficients. The recent-state exercise illustrates retrospective updating. The ranking has not been independently validated against observed deterioration, documented intervention urgency, or expert conservation priorities. Linking future screening rounds with field-inspection results and expert evaluations will provide the evidence for further calibration.

5. Conclusions

We present a digital twin-ready screening framework that combines official heritage records with dated environmental observations to establish repeatable inspection priorities. The Fujian application matches 914 traditional-village entries and 62 protected ancient buildings to 75 county-level areas, with 9900 county-month environmental observations spanning 2014–2024. Separate records of environmental pressure, heritage concentration, and tourism use make the screening score interpretable and suitable for subsequent updates.

Xiapu, Wuyishan, and Yongtai occupy the first three baseline positions for different combinations of the three screening components. The ranking is substantially concordant under alternative weights, environmental-domain tests, and the recent-state update; Monte Carlo draws describe the stability of the leading inspection candidates. The different component profiles provide a practical reason to examine both overall rank and its supporting evidence when planning field visits.

The framework connects provincial screening with county verification and specialist digital surveys, allowing selected locations to proceed to detailed HBIM-based diagnosis. Persistent identifiers and dated source records retain the evidence behind each inspection priority and support a repeatable, accountable sequence of conservation assessments across dispersed heritage portfolios.

Author Contributions: Conceptualization, H.T. and J.Z.; methodology, H.T. and J.Z.; software and formal analysis, H.T.; data curation, H.T.; investigation, H.T. and J.Z.; writing—original draft preparation, H.T.; writing—review and editing, H.T. and J.Z.; visualization, H.T.; supervision, J.Z.; project administration, H.T.; funding acquisition, H.T. All authors have read and agreed to the published version of the manuscript.

Funding: This research was funded by the 2025 Young and Middle-Aged Teacher Education Research Project (Science and Technology) of the Fujian Provincial Department of Education, "Theoretical Framework and Engineering Practice of Precision Restoration of Ancient Buildings Enabled by Digital Twin Technology", grant number JAT251281 (Min Jiao Ke (2025) No. 18).

Data Availability Statement: Analysis code and derived data used in this study are available from the author on reasonable request.

Acknowledgments: The authors acknowledge the public agencies and scientific data services whose published records underpin the heritage inventory and environmental indicators.

Conflicts of Interest: The authors declare no conflicts of interest.

Appendix A

Table A1. Heritage inventory and exposure score for the 75 matched counties.

County	Village Records	Ancient Buildings	Total Entries	Exposure Score	Tourism Observed
Yongtai County	47	0	47	0.987	No
Fuan City	45	0	45	0.947	Yes

Table A1. *Cont.*

County	Village Records	Ancient Buildings	Total Entries	Exposure Score	Tourism Observed
Yongding District	34	1	35	0.967	Yes
Minqing County	34	1	35	0.967	Yes
Jiaocheng District	34	0	34	0.867	Yes
Nanjing County	31	1	32	0.907	Yes
Gutian County	30	2	32	1.000	Yes
Youxi County	30	1	31	0.893	Yes
Dehua County	26	2	28	0.927	No
Zhangping City	26	2	28	0.927	Yes
Liancheng County	26	0	26	0.787	Yes
Zhenghe County	24	0	24	0.773	No
Datian County	23	0	23	0.760	No
Yanping District	22	1	23	0.840	Yes
Zhouzhu County	22	0	22	0.747	Yes
Xiapu County	19	3	22	0.880	Yes
Yongan City	20	1	21	0.827	Yes
Pingnan County	20	0	20	0.693	Yes
Shouzhu County	19	0	19	0.647	Yes
Jianou City	14	5	19	0.853	No
Pucheng County	19	0	19	0.647	No
Anxi County	16	2	18	0.807	Yes
Wuyishan City	16	2	18	0.807	Yes
Yongchun County	15	1	16	0.720	Yes
Shanghang County	14	1	15	0.667	Yes
Taizhu County	7	8	15	0.707	No
Shunchang County	13	2	15	0.733	Yes
Fuding City	13	0	13	0.600	Yes
Changting County	9	4	13	0.680	Yes
Guangze County	12	0	12	0.513	Yes
Songxi County	12	0	12	0.513	Yes
Xinluo District	10	1	11	0.627	Yes
Luoyuan County	11	0	11	0.467	Yes
Nanan City	9	1	10	0.580	Yes
Pinghe County	8	2	10	0.613	No
Zherong County	10	0	10	0.453	No
Shaowu City	9	1	10	0.580	Yes
Xianyou County	6	3	9	0.533	No
Huaan County	8	1	9	0.487	Yes
Zhuhua County	8	1	9	0.487	Yes
Wuping County	9	0	9	0.433	Yes
Quangang District	7	2	9	0.553	Yes
Fuqing City	9	0	9	0.433	Yes
Changtai District	7	2	9	0.553	Yes
Pingtan County	8	0	8	0.400	Yes
Sanyuan District	5	2	7	0.413	No
Yunxiao County	7	0	7	0.347	Yes
Hanjiang District	7	0	7	0.347	No
Lianjiang County	7	0	7	0.347	No
Dongshan County	5	1	6	0.380	Yes
Jianzhu County	5	1	6	0.380	No
Jianyang District	6	0	6	0.320	No
Jiangle County	5	0	5	0.280	No
Jinjiang City	5	0	5	0.280	Yes
Shaxian District	5	0	5	0.280	Yes
Qingliu County	5	0	5	0.280	Yes
Zhaoan County	5	0	5	0.280	No
Mingxi County	4	0	4	0.233	Yes
Luojiang District	4	0	4	0.233	Yes
Chengxiang District	3	0	3	0.173	No
Huian County	3	0	3	0.173	Yes

Table A1. *Cont.*

County	Village Records	Ancient Buildings	Total Entries	Exposure Score	Tourism Observed
Zhangpu County	3	0	3	0.173	No
Shishi City	3	0	3	0.173	No
Xiangan District	2	1	3	0.213	No
Licheng District	3	0	3	0.173	Yes
Fengze District	1	1	2	0.100	No
Jinan District	1	1	2	0.100	No
Changle District	2	0	2	0.127	Yes
Minhou County	2	0	2	0.127	Yes
Tongan District	1	0	1	0.053	No
Haicang District	1	0	1	0.053	Yes
Xiuyu District	1	0	1	0.053	No
Xiangcheng District	1	0	1	0.053	Yes
Jimei District	1	0	1	0.053	Yes
Longhai District	0	1	1	0.013	Yes

Note: Traditional-village values are official provincial list records. Ancient buildings are from the eleventh provincial protection batch.

Table A2. Environmental-state thresholds and compound indicators.

State	Definition	Pooled Fujian Threshold	Role
Extreme wind	Wind $\geq$ 90th percentile	2.999 m s^{-1}	Monthly binary state
Extreme rain	Precipitation $\geq$ 90th percentile	294.085 mm	Monthly binary state
Extreme heat	Temperature $\geq$ 90th percentile	26.926 °C	Monthly binary state
Vegetation stress	NDVI $\leq$ 10th percentile	0.496	Monthly binary state
Wind–rain concurrence	Extreme wind $\times$ extreme rain	—	Joint monthly state
Heat–rain concurrence	Extreme heat $\times$ extreme rain	—	Joint monthly state

Note: Thresholds are calculated from the 2014–2024 Fujian county-month observations after excluding Kinmen. The NDVI threshold is reported after applying the MOD13A3 scale factor of 0.0001.

Table A3. Component diagnostics for the baseline top 25 counties.

Rank	County	Wind	Rain	Heat–Wet	Env. Stress	Heritage	Tourism	Priority
1	Xiapu County	0.642	0.508	0.692	0.465	0.880	0.840	0.722
2	Wuyishan City	0.399	0.794	0.358	0.503	0.807	1.000	0.689
3	Yongtai County	0.399	0.651	0.329	0.487	0.987	0.510	0.655
4	Nanjing County	0.399	0.590	0.263	0.225	0.907	0.900	0.637
5	Yanping District	0.399	0.304	0.575	0.508	0.840	0.780	0.634
6	Fuqing City	0.923	0.589	0.754	0.721	0.433	0.720	0.633
7	Jiaocheng District	0.399	0.742	0.329	0.380	0.867	0.640	0.631
8	Fuding City	0.399	0.694	0.648	0.481	0.600	0.920	0.626
9	Fuan City	0.399	0.421	0.358	0.289	0.947	0.700	0.620
10	Jianou City	0.399	0.421	0.553	0.535	0.853	0.510	0.614
11	Taizhu County	0.399	0.742	0.435	0.711	0.707	0.510	0.610
12	Nanan City	0.642	0.590	0.538	0.492	0.580	0.820	0.609
13	Shunchang County	0.399	0.508	0.575	0.881	0.733	0.360	0.606
14	Jinjiang City	0.776	0.248	0.936	0.915	0.280	0.980	0.604
15	Dehua County	0.399	0.590	0.193	0.412	0.927	0.510	0.600
16	Dongshan County	0.768	0.356	0.973	0.513	0.380	0.880	0.591
17	Quangang District	0.716	0.651	0.813	0.904	0.553	0.080	0.591
18	Shaowu City	0.399	0.776	0.505	0.593	0.580	0.620	0.580
19	Pucheng County	0.399	0.785	0.479	0.540	0.647	0.510	0.578
20	Yongding District	0.399	0.213	0.263	0.247	0.967	0.660	0.578
21	Pingtan County	1.000	0.437	0.893	0.188	0.400	0.800	0.575
22	Gutian County	0.399	0.356	0.329	0.295	1.000	0.340	0.573
23	Changting County	0.399	0.421	0.406	0.599	0.680	0.680	0.568
24	Zhenghe County	0.399	0.742	0.307	0.316	0.773	0.510	0.568
25	Anxi County	0.399	0.508	0.263	0.193	0.807	0.740	0.564

Note: All component scores are percentile-based and bounded between 0 and 1.

Table A4. Monte Carlo rank uncertainty for the baseline top 25.

Baseline Rank	County	Median Rank	P05	P95	P(top 10)	P(top 20)
1	Xiapu County	1	1	1	100.0%	100.0%
2	Wuyishan City	2	2	4	99.7%	100.0%
3	Yongtai County	4	2	14	90.1%	99.1%
4	Nanjing County	6	3	22	72.9%	93.7%
5	Yanping District	7	5	16	83.9%	98.1%
6	Fuqing City	7	2	23	69.4%	91.8%
7	Jiaocheng District	7	4	16	75.9%	97.4%
8	Fuding City	8	4	17	66.7%	98.7%
9	Fuan City	10	5	26	52.2%	86.2%
10	Jianou City	11	8	22	46.2%	92.8%
11	Taizhu County	13	8	17	14.1%	99.2%
12	Nanan City	13	8	21	31.4%	94.2%
13	Shunchang County	14	6	23	26.9%	91.3%
14	Jinjiang City	13	3	34	43.0%	72.6%
15	Dehua County	15	8	29	26.7%	74.1%
16	Dongshan County	16	6	32	20.9%	66.3%
17	Quangang District	17	3	34	27.8%	62.1%
18	Shaowu City	20	17	27	0.0%	62.0%
19	Pucheng County	21	17	26	0.0%	37.0%
20	Yongding District	20	9	41	9.7%	51.1%
21	Pingtan County	21	11	34	4.3%	46.2%
22	Gutian County	22	10	41	8.6%	45.2%
23	Changting County	24	21	28	0.0%	4.5%
24	Zhenghe County	24	19	32	0.0%	17.5%
25	Anxi County	26	15	38	0.0%	27.3%

Note: Results are from 10,000 Dirichlet weight draws centered on baseline outer weights (0.50, 0.35, 0.15).

Table A5. Largest rank changes after updating the environmental state to 2022–2024.

County	Long-Run Rank	Recent Rank	Δ Rank	Direction	Long-Run Score	Recent Score
Zhangpu County	63	50	−13	Higher priority	0.423	0.468
Anxi County	25	13	−12	Higher priority	0.564	0.600
Jimei District	36	24	−12	Higher priority	0.514	0.567
Zherong County	56	44	−12	Higher priority	0.437	0.490
Zhaoan County	59	47	−12	Higher priority	0.430	0.476
Haicang District	61	49	−12	Higher priority	0.424	0.469
Zhuhua County	64	52	−12	Higher priority	0.419	0.454
Yongding District	20	9	−11	Higher priority	0.578	0.620
Yunxiao County	68	58	−10	Higher priority	0.391	0.428
Xinluo District	32	23	−9	Higher priority	0.545	0.575
Jianou City	10	17	7	Lower priority	0.614	0.596
Chengxiang District	58	65	7	Lower priority	0.434	0.404
Changting County	23	32	9	Lower priority	0.568	0.540
Pucheng County	19	29	10	Lower priority	0.578	0.548
Xiangan District	34	45	11	Lower priority	0.522	0.484
Songxi County	49	63	14	Lower priority	0.470	0.410
Fengze District	51	66	15	Lower priority	0.458	0.397
Xiuyu District	41	57	16	Lower priority	0.491	0.432
Shaowu City	18	37	19	Lower priority	0.580	0.517
Jianyang District	45	64	19	Lower priority	0.486	0.410

Note: Negative Δ rank indicates movement toward higher inspection priority because rank 1 is the highest priority.

Table A6. Inspection-rank concordance under additional source and indicator sensitivity scenarios.

Scenario	Spearman ρ	Top-10 Overlap	Median Absolute Rank Shift
Missing tourism assigned to lower bound	0.934	8	5.0
Missing tourism assigned to upper bound	0.931	6	7.0
Excluding wind	0.980	8	3.0

Table A6. *Cont.*

Scenario	Spearman ρ	Top-10 Overlap	Median Absolute Rank Shift
Excluding heavy rain	0.922	6	5.0
Excluding heat–wet	0.968	7	3.0
Excluding environmental stress	0.968	9	3.0

Note: Tourism substitutions apply only to the 25 counties with missing reported tourism revenue. Environmental-domain exclusions renormalize the remaining three environmental domains to equal shares. Rank 1 denotes the highest inspection priority.

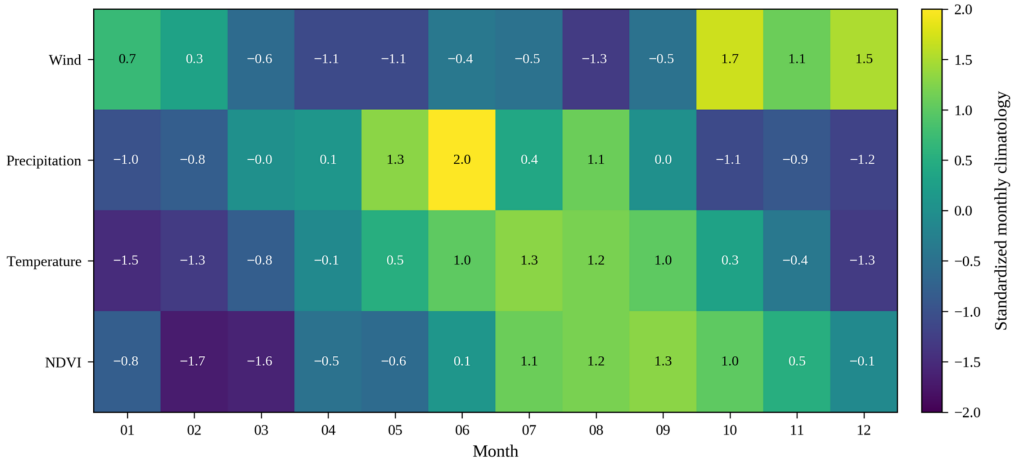


Figure A1. Standardized monthly climatology of ERA5-Land wind, precipitation, and temperature and MOD13A3 NDVI across Fujian, 2014–2024. Every heatmap cell reports the standardized monthly value.

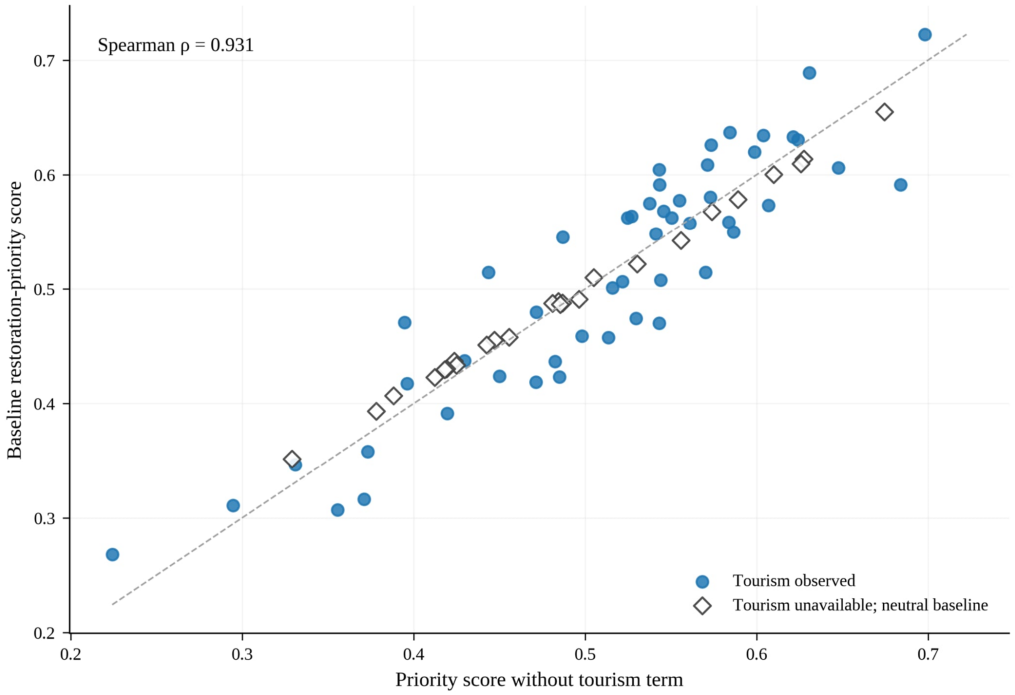


Figure A2. Baseline priority compared with a specification that omits tourism pressure. Marker type distinguishes counties with an observed tourism value from counties receiving the neutral median tourism state in the baseline.

$$\Delta r_i = r_i^{\text{recent}} - r_i^{\text{long-run}} \tag{A1}$$

$$\rho_s = 1 - \frac{6\sum_{i=1}^{N} d_i^2}{N(N^2-1)} \tag{A2}$$

References

1. Fatorić, S.; Seekamp, E. Are cultural heritage and resources threatened by climate change? A systematic literature review. *Clim. Change* **2017**, *142*, 227–254. [CrossRef]
2. Sesana, E.; Gagnon, A.S.; Ciantelli, C.; Cassar, J.A.; Hughes, J.J. Climate change impacts on cultural heritage: A literature review. *WIREs Clim. Change* **2021**, *12*, e710. [CrossRef]
3. Zscheischler, J.; Westra, S.; van den Hurk, B.J.J.M.; Seneviratne, S.I.; Ward, P.J.; Pitman, A.; AghaKouchak, A.; Bresch, D.N.; Leonard, M.; Wahl, T.; et al. Future climate risk from compound events. *Nat. Clim. Change* **2018**, *8*, 469–477. [CrossRef]
4. Gill, J.C.; Malamud, B.D. Reviewing and visualizing the interactions of natural hazards. *Rev. Geophys.* **2014**, *52*, 680–722. [CrossRef]
5. Tilloy, A.; Malamud, B.D.; Winter, H.; Joly-Laugel, A. A review of quantification methodologies for multi-hazard interrelationships. *Earth-Sci. Rev.* **2019**, *196*, 102881. [CrossRef]
6. Murphy, M.; McGovern, E.; Pavia, S. Historic building information modelling (HBIM). *Struct. Surv.* **2009**, *27*, 311–327. [CrossRef]
7. Murphy, M.; McGovern, E.; Pavia, S. Historic Building Information Modelling—Adding intelligence to laser and image based surveys of European classical architecture. *ISPRS J. Photogramm. Remote Sens.* **2013**, *76*, 89–102. [CrossRef]
8. Pepe, M.; Costantino, D.; Alfio, V.S.; Garofalo Restuccia, A.; Papalino, N.M. Scan to BIM for the digital management and representation in 3D GIS environment of cultural heritage site. *J. Cult. Herit.* **2021**, *50*, 115–125. [CrossRef]
9. Boje, C.; Guerriero, A.; Kubicki, S.; Rezgui, Y. Towards a semantic Construction Digital Twin: Directions for future research. *Autom. Constr.* **2020**, *114*, 103179. [CrossRef]
10. AlBalkhy, W.; Karmaoui, D.; Ducoulombier, L.; Lafhaj, Z.; Linner, T. Digital twins in the built environment: Definition, applications, and challenges. *Autom. Constr.* **2024**, *162*, 105368. [CrossRef]
11. Lauria, M.; Azzalin, M. Digital Twin Approach in Buildings: Future Challenges via a Critical Literature Review. *Buildings* **2024**, *14*, 376. [CrossRef]
12. Wang, Y.; García Valldecabres, J.L.; Escudero, P.A. HBIM and Digital Twin in Architectural Heritage: A Bibliometric Analysis and Future Research Directions. *Buildings* **2026**, *16*, 2762. [CrossRef]
13. Khan, M.S.; Khan, M.; Bughio, M.; Talpur, B.D.; Kim, I.S.; Seo, J. An Integrated HBIM Framework for the Management of Heritage Buildings. *Buildings* **2022**, *12*, 964. [CrossRef]
14. Liu, J.; Foreman, G.; Sattineni, A.; Li, B. Integrating Stakeholders' Priorities into Level of Development Supplemental Guidelines for HBIM Implementation. *Buildings* **2023**, *13*, 530. [CrossRef]
15. Kong, X.; Hucks, R.G. Preserving our heritage: A photogrammetry-based digital twin framework for monitoring deteriorations of historic structures. *Autom. Constr.* **2023**, *152*, 104928. [CrossRef]
16. Hosamo, H.; Mazzetto, S. Integrating Knowledge Graphs and Digital Twins for Heritage Building Conservation. *Buildings* **2025**, *15*, 16. [CrossRef]
17. Wang, G.; Wang, Y.; Guo, M.; Liang, X.; Fu, Y.; Li, H. Research on Value-Chain-Driven Multi-Level Digital Twin Models for Architectural Heritage. *Buildings* **2025**, *15*, 2984. [CrossRef]
18. Meriggi, P.; Bianchini Ciampoli, L. V-HBIM: A Vulnerability-Oriented Heritage BIM Workflow for Cultural Heritage Conservation. *Buildings* **2026**, *16*, 2570. [CrossRef]
19. Massafra, A.; Coraglia, U.M.; Di Turi, S.; Palladino, D. Federated Data Modelling for Heritage Building Performance Management. *Buildings* **2026**, *16*, 27. [CrossRef]
20. Zhao, Y.; Li, K.; Zhang, W. Digital Twin–Based Simulation and Decision-Making Framework for the Renewal Design of Urban Industrial Heritage Buildings and Environments: A Case Study of the Xi'an Old Steel Plant Industrial Park. *Buildings* **2025**, *15*, 4367. [CrossRef]
21. Ma, Y.; Zhang, Q.; Huang, L. Spatial distribution characteristics and influencing factors of traditional villages in Fujian Province, China. *Humanit. Soc. Sci. Commun.* **2023**, *10*, 883. [CrossRef]
22. Chen, W.; Yang, Z.; Yang, L.; Wu, J.; Bian, J.; Zeng, J.; Liu, Z. Identifying the spatial differentiation factors of traditional villages in China. *Herit. Sci.* **2023**, *11*, 149. [CrossRef]
23. Liu, W.; Xue, Y.; Shang, C. Spatial distribution analysis and driving factors of traditional villages in Henan province: A comprehensive approach via geospatial techniques and statistical models. *Herit. Sci.* **2023**, *11*, 185. [CrossRef]

24. Ma, H.; Tong, Y. Spatial differentiation of traditional villages using ArcGIS and GeoDa: A case study of Southwest China. *Ecol. Inform.* **2022**, *68*, 101416. [CrossRef]
25. Gao, J.; Wu, B. Revitalizing traditional villages through rural tourism: A case study of Yuanjia Village, Shaanxi Province, China. *Tour. Manag.* **2017**, *63*, 223–233. [CrossRef]
26. Hersbach, H.; Bell, B.; Berrisford, P.; Hirahara, S.; Horányi, A.; Muñoz-Sabater, J.; Nicolas, J.; Peubey, C.; Radu, R.; Schepers, D.; et al. The ERA5 global reanalysis. *Q. J. R. Meteorol. Soc.* **2020**, *146*, 1999–2049. [CrossRef]
27. Muñoz-Sabater, J.; Dutra, E.; Agustí-Panareda, A.; Albergel, C.; Arduini, G.; Balsamo, G.; Boussetta, S.; Choulga, M.; Harrigan, S.; Hersbach, H.; et al. ERA5-Land: A state-of-the-art global reanalysis dataset for land applications. *Earth Syst. Sci. Data* **2021**, *13*, 4349–4383. [CrossRef]
28. Huete, A.; Didan, K.; Miura, T.; Rodriguez, E.P.; Gao, X.; Ferreira, L.G. Overview of the radiometric and biophysical performance of the MODIS vegetation indices. *Remote Sens. Environ.* **2002**, *83*, 195–213. [CrossRef]
29. Hyndman, R.J.; Fan, Y. Sample quantiles in statistical packages. *Am. Stat.* **1996**, *50*, 361–365. [CrossRef]
30. Spearman, C. The proof and measurement of association between two things. *Am. J. Psychol.* **1904**, *15*, 72–101. [CrossRef]
31. Greco, S.; Ishizaka, A.; Tasiou, M.; Torrisi, G. On the methodological framework of composite indices: A review of the issues of weighting, aggregation, and robustness. *Soc. Indic. Res.* **2019**, *141*, 61–94. [CrossRef]
32. Helton, J.C.; Davis, F.J. Latin hypercube sampling and the propagation of uncertainty in analyses of complex systems. *Reliab. Eng. Syst. Saf.* **2003**, *81*, 23–69. [CrossRef]
33. Saltelli, A.; Annoni, P.; Azzini, I.; Campolongo, F.; Ratto, M.; Tarantola, S. Variance based sensitivity analysis of model output. Design and estimator for the total sensitivity index. *Comput. Phys. Commun.* **2010**, *181*, 259–270. [CrossRef]
34. Saisana, M.; Saltelli, A.; Tarantola, S. Uncertainty and sensitivity analysis techniques as tools for the quality assessment of composite indicators. *J. R. Stat. Soc. Ser. A Stat. Soc.* **2005**, *168*, 307–323. [CrossRef]
35. Willkens, D.S.; Liu, J.; Alathamneh, S. A Case Study of Integrating Terrestrial Laser Scanning (TLS) and Building Information Modeling (BIM) in Heritage Bridge Documentation: The Edmund Pettus Bridge. *Buildings* **2024**, *14*, 1940. [CrossRef]
36. Bonaguidi, L.; Sebastiani, C.; Santini, S. Sustainable Seismic Energy Assessment of Italian Residential Heritage in Reinforced Concrete with Masonry Infills: An HBIM Evaluation Tool. *Buildings* **2024**, *14*, 4050. [CrossRef]
37. Christoforou, E.; Klitou, T.; Douni, O.; Apostolidou, E.; Afxentiou, N.; Schetakis, N.; Xekalakis, G.; Christou, P.; Di Iorio, A.; Stavroulakis, G.; et al. From Crowdsourcing to TLS–BIM/HBIM Workflows for Cultural Heritage Documentation and Structural Assessment: A Review. *Buildings* **2026**, *16*, 3066. [CrossRef]
38. Koks, E.E.; Rozenberg, J.; Zorn, C.; Tariverdi, M.; Vousdoukas, M.; Fraser, S.A.; Hall, J.W.; Hallegatte, S. A global multi-hazard risk analysis of road and railway infrastructure assets. *Nat. Commun.* **2019**, *10*, 2677. [CrossRef]
39. Salazar, L.G.F.; Figueiredo, R.; Romão, X. Flood vulnerability assessment of built cultural heritage: Literature review and identification of indicators. *Int. J. Disaster Risk Reduct.* **2024**, *111*, 104666. [CrossRef]
40. Lei, T.; Wang, J.; Jiang, Y.; Sun, S.; Simpson, N.P.; Pang, X.; Shen, B.; Wu, Y.; Wu, Y.; Wang, Q.; et al. Climate risk assessment of China's Cultural World Heritage highlights urgent need for adaptation. *npj Herit. Sci.* **2026**, *14*, 257. [CrossRef]
41. Phillips, H. The capacity to adapt to climate change at heritage sites—The development of a conceptual framework. *Environ. Sci. Policy* **2015**, *47*, 118–125. [CrossRef]
42. Reimann, L.; Vafeidis, A.T.; Brown, S.; Hinkel, J.; Tol, R.S.J. Mediterranean UNESCO World Heritage at risk from coastal flooding and erosion due to sea-level rise. *Nat. Commun.* **2018**, *9*, 4161. [CrossRef]
43. Durrant, L.J.; Vadher, A.N.; Teller, J. Disaster risk management and cultural heritage: The perceptions of European world heritage site managers on disaster risk management. *Int. J. Disaster Risk Reduct.* **2023**, *89*, 103625. [CrossRef]
44. Aktürk, G.; Hauser, S.J. Integrated understanding of climate change and disaster risk for building resilience of cultural heritage sites. *Nat. Hazards* **2025**, *121*, 4309–4334. [CrossRef]
45. Torres, R.; Snoeij, P.; Geudtner, D.; Bibby, D.; Davidson, M.; Attema, E.; Potin, P.; Rommen, B.; Floury, N.; Brown, M.; et al. GMES Sentinel-1 mission. *Remote Sens. Environ.* **2012**, *120*, 9–24. [CrossRef]
46. Brown, C.F.; Brumby, S.P.; Guzder-Williams, B.; Birch, T.; Hyde, S.B.; Mazzariello, J.; Czerwinski, W.; Pasquarella, V.J.; Haertel, R.; Ilyushchenko, S.; et al. Dynamic World, Near real-time global 10 m land use land cover mapping. *Sci. Data* **2022**, *9*, 251. [CrossRef]
47. Gorelick, N.; Hancher, M.; Dixon, M.; Ilyushchenko, S.; Thau, D.; Moore, R. Google Earth Engine: Planetary-scale geospatial analysis for everyone. *Remote Sens. Environ.* **2017**, *202*, 18–27. [CrossRef]
48. Pekel, J.-F.; Cottam, A.; Gorelick, N.; Belward, A.S. High-resolution mapping of global surface water and its long-term changes. *Nature* **2016**, *540*, 418–422. [CrossRef] [PubMed]
49. Knapp, K.R.; Kruk, M.C.; Levinson, D.H.; Diamond, H.J.; Neumann, C.J. The International Best Track Archive for Climate Stewardship (IBTrACS): Unifying tropical cyclone best track data. *Bull. Am. Meteorol. Soc.* **2010**, *91*, 363–376. [CrossRef]
50. Pocobelli, D.P.; Boehm, J.; Bryan, P.; Still, J.; Grau-Bové, J. BIM for heritage science: A review. *Herit. Sci.* **2018**, *6*, 30. [CrossRef]

51. Sevieri, G.; Galasso, C.; D'Ayala, D.; De Jesus, R.; Oreta, A.; Grio, M.E.D.A.; Ibabao, R. A Multi-Hazard Risk Prioritisation Framework for Cultural Heritage Assets. *Nat. Hazards Earth Syst. Sci.* **2020**, *20*, 1391–1414. [CrossRef]
52. Sugiyama, G.; Bourgeois, I.; Rodrigues, H. A Holistic Methodology for the Assessment of Heritage Digital Twin Applied to Portuguese Case Studies. *Digit. Appl. Archaeol. Cult. Herit.* **2025**, *36*, e00390. [CrossRef]

Disclaimer/Publisher's Note: The statements, opinions and data contained in all publications are solely those of the individual author(s) and contributor(s) and not of MDPI and/or the editor(s). MDPI and/or the editor(s) disclaim responsibility for any injury to people or property resulting from any ideas, methods, instructions or products referred to in the content.